An investigation into the Zeeman Effect.

Maxim Beekenkamp
Brown University
June 1, 2022

***Abstract* – The Zeeman Effect has great theoretical importance, allowing us to look at the affect of an intrinsic quantum mechanical property, spin, on the atomic energy levels; but being one of the primary principles in MRIs it also has practical significance. In this lab, we study two methods of measuring wavelength; primarily by changing the distance between the mirrors of our Fabry-Pérot interferometer, and secondly by changing the angle from the normal of the light as it enters our Fabry-Pérot interferometer; and the splitting of spectral lines in the presence of a magnetic field.**

I. INTRODUCTION

In 1896, whilst teaching at the University of Leiden, the Dutch Physicist Pieter Zeeman discovered the Zeeman Effect for which he would later win a Nobel Prize. Based on Lorentz's theory of electromagnetic radiation, for whom Zeeman had TA'ed as an undergraduate student, Zeeman noted the splitting of spectral lines under the presence of a large magnetic field. This discovery confirmed Lorentz's theory on polarised light and showed the presence of the electron, although it would take a further year before the it was discovered by J.J. Thomson. An example of such spectral lines, and it's splitting, is shown in Fig.1 & 2 respectively.

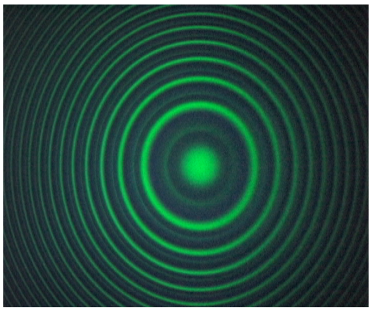

Fig. 1. Example of spectral lines [2]

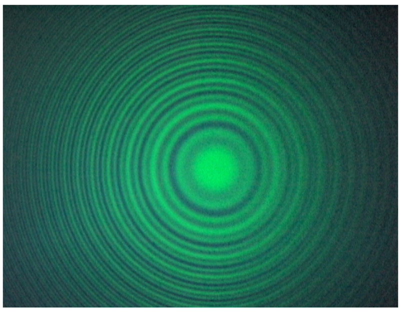

Fig. 2. Example of spectral lines under the presence of a magnetic field [2]

A current passing through a mercury discharge tube ionises electrons in the mercury causing photon emission. This leaves a space for an electron from an outer shell to fall into the vacancy left by the ionised electron. The act of the electron dropping emits quantised photons with an energy equivalent to the energy level unique to each element. This can be seen in Fig.3. These emitted photons are the spectral lines shown in Fig.1.

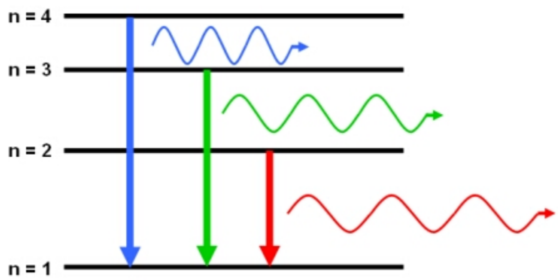

Fig. 3. Example of quantised atomic energy levels [1]

Under a magnetic field these emitted photons split. The Planck-Einstein relation (1) is a fundamental equation stating that photon energy is proportional to its frequency. As the Zeeman interaction causes a change in energy (7), it also changes the frequency of the emitted photons. This change in frequency is what is observed in experimentally (Fig.2).

$$E = hf \tag{1}$$

Where:
- E - photon energy;
- h - Planck's constant;
- f - frequency.

The selection rules are restrictions on splitting due to conservation rules on the system. The electron transition which results in photon emission must also have a change of 1 in the angular momentum. As the photon has a spin of 1, and angular momentum in the system must be conserved, the atom's angular momentum an intrinsic angular momentum or "spin" of one, so that conservation of angular momentum in photon emission requires a change of 1 in the atom's angular momentum. This yields the first selection rule (2):

$$\Delta m_s = 0 \tag{2}$$

Where:
- Δm_s - change in electron spin quantum number.

Similarly the photon emission is accompanied by a change of 1 in the orbital angular momentum quantum number and a change by 0 or 1 in the magnetic quantum number. These yield the second (3) and third (4) selection rules, combining into Eq.5:

$$\Delta l = \pm 1 \tag{3}$$

$$\Delta m_l = 0,\ \pm 1 \tag{4}$$

Where:

Δl - change in orbital angular momentum quantum number.

Δm_l - change in magnetic quantum number.

$$\Delta j = 0,\ \pm 1 \tag{5}$$

$$\Delta j = l \pm s\ = l \pm \frac{1}{2} \tag{6}$$

Where:

Δj - change in total angular momentum quantum number.

The Zeeman interaction, the interaction energy of an electron with a magnetic field, is thus defined by (7):

$$\Delta E = \frac{e}{2m_e}(\vec{L} + 2\vec{S})\vec{B} = g_L \mu_B m_j B \tag{7}$$

$$\mu_B = \frac{e\hbar}{2m_e} \tag{8}$$

Where:

ΔE - change in total energy;
e - charge of an electron;
m_e - mass of an electron;
$\vec{L}$ - orbital angular momentum;
$\vec{S}$ - spin angular momentum;
$\vec{B}$ - magnetic field;
g_L - Landé g-factor;
μ_B - Bohr magnetron;
$\hbar$ - reduced Plank's constant.

From (6)

$$J = \sqrt{j(j+1)}\hbar \tag{9}$$

The $\hat{z}$-component of the total angular momentum is

$$J_z = m_j \hbar, m_j = -j, -j+1, \ldots, j-1, j \tag{10}$$

Meaning a magnetic field causes a single energy level to split into $2J+1$ components. This experiment analyses the $7S \rightarrow 6P$ atomic transition in mercury. The $7S$ energy level ($J = 1, L = 0, S = 1$) splits into three components and the $6P$ energy level ($J = 2, L = 1, S = 1$) splits into five. To calculate the Landé g-factor for these energy levels Eq.11 is used:

$$g_L = 1 + \frac{j(j+1) + s(s+1) - l(l+1)}{2j(j+1)} \tag{11}$$

Resulting in $g_{7S} = 2$ and $g_{6P} = \frac{3}{2}$. These splittings are shown in Fig.4. In this experiment the focus is on the π transitions. As σ transitions are polarised at 90° relative to the magnetic field they can be blocked, with the use of a polariser, whilst allowing the π transitions to pass through. Visually, in reference to Fig.4, the transitions analysed in this experiment are $m_j = 0; g = 2 \rightarrow m_j = 0, \pm 1; g = \frac{3}{2}$. The equation governing the energy shifts of the π transitions is:

$$\Delta E = 0,\ \pm \frac{1}{2}\mu_B B \tag{12}$$

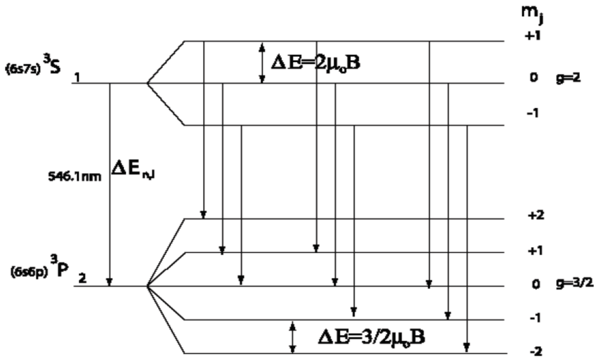

Fig. 4. Energy levels diagram for $7S \rightarrow 6P$ splitting [2]

Using a Fabry-Pérot interferometer, the change in frequency of the Zeeman Effect is observed (Eq.1 & 12). Light passing through the Fabry-Pérot interferometer will interfere constructively according to Eq.13:

$$2d\cos\theta = n\lambda \tag{13}$$

Where:

d - distance between mirrors of the Fabry-Pérot interferometer;
θ - angle from normal of incoming light;
n - integer of the ring order;
λ - wavelength.

Following small angle approximations, which are valid due to the fine nature of this experiment, we get Eq.14 & 15:

$$n \approx \frac{2d}{\lambda} \tag{14}$$

$$\theta_p^2 = (p + \varepsilon)\frac{\lambda}{d} \tag{15}$$

$$p = n_0 - n, \quad 0 \leq \varepsilon \leq 1 \tag{16}$$

Where:

ε - correction factor.

II. EXPERIMENT

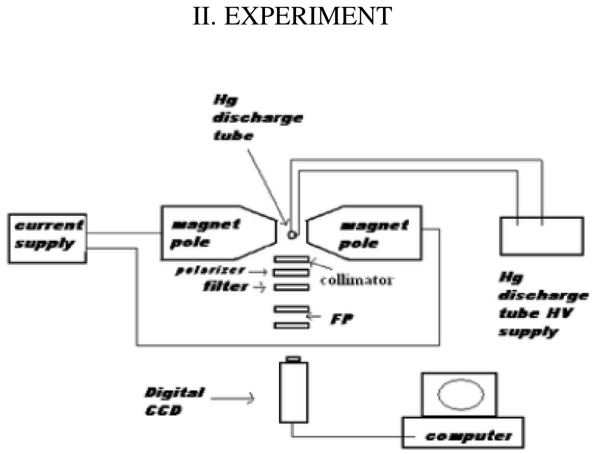

Fig. 5. A schematic of the Fabry-Pérot interferometer [2]

The experiment had two parts, studying spectral lines and the Zeeman Effect. For both parts "VirtualDub" was used to display the spectral lines on a computer as shown in Fig.5.

A. Spectral Lines

1) Measuring Wavelength by Spacing: Once viewing the spectral lines we rotated the micrometer, increasing the distance between the mirrors, counting 20 rings which passed the edge of a fixed point. We chose to open a blank notepad window to use as a reference. This was repeated for each of the ten readings. This method does not require any knowledge about the initial conditions of the Fabry-Pérot interferometer only the relative change induced by the micrometer.

TABLE I
Counting Rings with Micrometer

Number of Rings	**Increment** (mm)
0	0
20 ± 1	0.02 ± 0.005
40± 1	0.04± 0.005
60 ± 1	0.6 ± 0.005
80± 1	0.9 ± 0.005
100 ± 1	0.11± 0.005
120 ± 1	0.13± 0.005
140 ± 1	0.15 ± 0.005
160 ± 1	0.16± 0.005
180± 1	0.18 ± 0.005
200 ± 1	0.19± 0.005

2) Measuring Wavelength by Angle: Here, instead of looking at the effect of an increase in distance, we measured the effect of a change of angle. By aligning the outermost ring, which was still clearly differentiable, with the edge of the screen, and rotating the camera we measured the spacing between each ring. Once again this method does not require any knowledge about the initial conditions of the Fabry-Pérot interferometer.

TABLE II
Counting Rings with Angle

Ring Order	**Left Side Angle** ($\frac{1}{60}$ deg)	**Right Side Angle** ($\frac{1}{60}$ deg)
0	17	62
1	26 ± 1	53 ± 1
2	34± 1	44 ± 1
3	40 ± 1	39 ± 1
4	47 ± 1	31 ± 1
5	53± 1	24 ± 1

B. Zeeman Splitting

For experiment B we are looking at the effect a B-Field has on the spectral lines. At $0.2A$ intervals one second videos were taken of the observed spectral lines using "VirtualDub". Using "ImageJ" the approximately 30 frames were averaged and created a horizontal profile plot. For each B-Field we measured the average wavelength shift caused by the Zeeman effect.

TABLE III
Strength of Magnetic Field

Current (A)	**Voltage** (V)
0	0
0.2 ± 0.05	4.9 ± 0.05
0.4± 0.05	9.7± 0.05
0.6 ± 0.05	14.5 ± 0.05
0.8± 0.05	19.5 ± 0.05
1.0 ± 0.05	24.2± 0.05
1.2 ± 0.05	25.8± 0.05

III. RESULTS AND ANALYSIS

A. Spectral Lines

1) Measuring Wavelength by Spacing: The data obtained in Table I displays the relationship defined in Eq.14. Specifically, the linear relationship between distance d and the wavelength. After obtaining the data shown in Table I, using Eq.14 the wavelength of green light emitted from the mercury vapour was calculated. Graphically, as shown in Fig.6, this is the gradient of the linear regression.

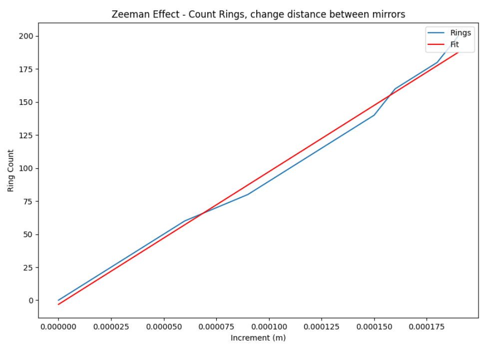

Fig. 6. The linear relationship between n, the Ring Count and d the Increment. The gradient is $\frac{2}{\lambda}$.

2) Measuring Wavelength with Angle: Here, using Eq.15 and the data in Table II, the linear relationship between θ^2 and p is shown in Fig.7. The gradient of the linear regression is again the wavelength of the green light emitted from the mercury vapour.

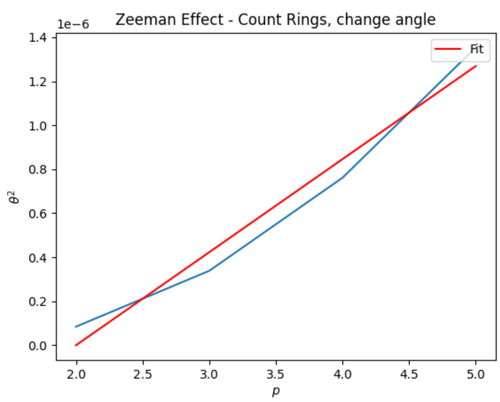

Fig. 7. The linear relationship between θ^2, the angle of the incoming light and p the relative ring order number. The gradient is $\frac{\lambda}{d}$.

The resulting wavelengths and their errors are listed in Table IV.

TABLE IV
Results from Experiment A

Experiment	Wavelength λ, (nm)	Error
Theoretical	546.1	-
Experiment 1	498.0 $\pm$176.2	8.81%
Experiment 2	423.1 $\pm$231.7	22.52%

Both of the experimental values for wavelength have the correct order of magnitude. Given the possible errors from difficulty operating the lab equipment, most notably the dials to change d and θ not providing fine enough control, and the lack of knowledge about our initial conditions, the result matches the theoretical expectations.

B. Zeeman Splitting

Seven scans were done in this experiment, shown in Table III. Each scan produced an averaged horizontal profile plot (HPFP) showing the intensity for each pixel of a line along the middle of images such as the ones seen in Fig.1 & 2.

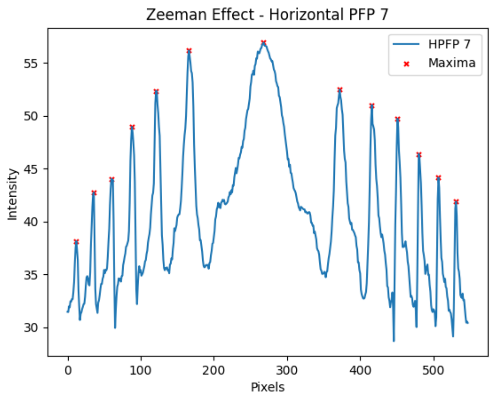

Fig. 8. Zeeman Splitting at 0 A.

To find the relationship described in the Zeeman effect, Eq.12., the peaks of the HPFPs were found using the Scipy function "find_peaks". This is shown in Fig.8 & 9. As the B-Field increased however, there was the find_peaks function created a lot of noise, shown in Fig.9, calling for some data cleansing.

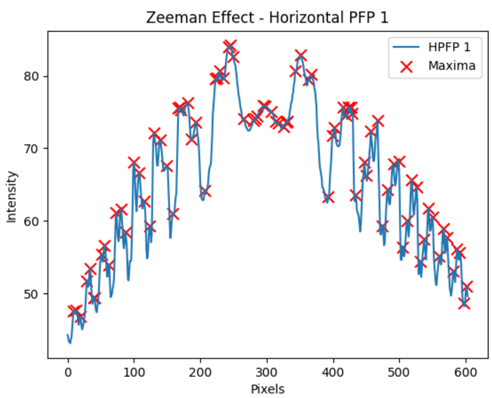

Fig. 9. Zeeman Splitting at 1.2 A.

Having found these peaks, we measured the wavelength shift (in pixels), left and right, from the central peak. These values were subsequently converted to metres using Eq.17, and used as the data set for Fig.10.

$$r = \frac{\lambda}{P} \tag{17}$$

Where:

r - conversion factor;
λ - wavelength;
P - average spacing between peaks in Fig.8 in pixels.

As the strength of the magnetic field remains linearly proportional to current for Helmholtz Coils, and because we could not measure the actual strength of the magnet, we used the current as the independent variable shown in Fig.10.

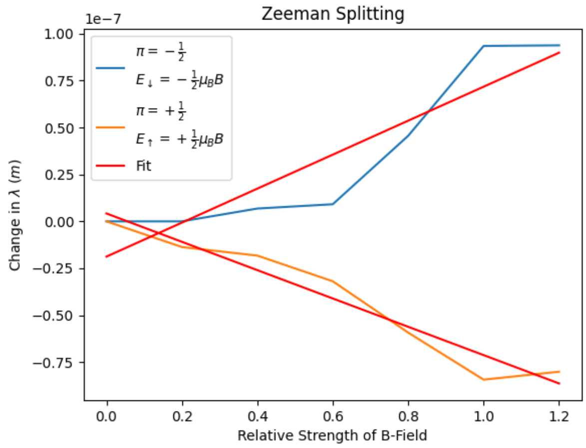

Fig. 10. The Zeeman Effect. The gradient of the slope is defined by the magnetic moment.

The resulting energy shifts and their errors are listed in Table V.

TABLE V
Results from Experiment B

Experiment	Magnetic Moment $J \cdot T^{-1}$)	Error
Theoretical	$\pm 4.637 \cdot 10^{-24}$	-
$E_\uparrow$	$+1.692 \cdot 10^{-18}$	n/a
$E_\downarrow$	$-1.692 \cdot 10^{-18}$	n/a

The observed experimental result does not accurately reproduce Zeeman's findings. However, the results are internally consistent, the gradient of both the spin up and spin down π readings are the same, indicating that there was a systematic error in our work. This is likely due to an incorrect pixel to metre conversion calculation.

IV. CONCLUSIONS

In this lab experiment, we were able to investigate the Zeeman effect. Specifically, Zeeman splitting was measured using computer software and the Fabry-Pérot interferometer. Using two different methods to calculate wavelength, we demonstrated the multiple practical ways to measure wavelengths each relying on seperate measurements. These experimental values had the correct order of magnitudes, however, large simplifications and assumptions undoubtedly limited the potential accuracy of our results. Considering the equipment's limitation and uncertainty, it is a very good result. Finally, Zeeman Splitting was demonstrated by measuring how the presence of a B-Field shifted the wavelength. Although the experimental value of the gradient of the linear regression shown in Fig.10 was internally consistent, the experimental value of this gradient failed to effectively support Zeeman's findings.

References

[1] *Emission Line*. URL: https://astronomy.swin.edu.au/cosmos/e/emission+line. (Accessed: 06/01/2022).

[2] DGH Stephen Albright JS. *Lab Manual*. URL: https://canvas.brown.edu/courses/1087786/files/folder/Lab_Manuals?preview=64797733. (Accessed: 06/01/2022).